PHYSICAL REVIEW D **86,** 072003 (2012)

Role of the Lower Positive Charge Region (LPCR) in initiation of the Thunderstorm Ground Enhancements (TGEs)

A. Chilingarian* and H. Mkrtchyan

Yerevan Physics Institute, Alikhanyan Brothers 2, Yerevan, Armenia

(Received 24 May 2012; published 8 October 2012)

Despite the ubiquity of thunderstorms, lightning, and related electrical phenomena, many important electromagnetic processes in our atmosphere are poorly understood; the key questions about the thundercloud electrification and lightning initiation remain unanswered. The bulk information on particle fluxes correlated with thunderstorm can be used to better understand the electrical structure of thunderclouds. Only very specific electric configuration of the lower part of the cloud can support the sustainable acceleration of the electrons. Our analysis is based on the thunderstorm data from the Aragats Mountain in Armenia, 3200 m above sea level Varieties of particle detectors located at Aragats Space Environmental Center are registering neutral and charged particle fluxes correlated with thunderstorms, so-called Thunderstorm Ground Enhancements (TGEs). Simultaneously the electrical mills and lightning detectors are monitoring the near-surface electric field and type of lightning occurrences; weather stations are measuring plenty of meteorological parameters. In the present paper we relate particle fluxes to the electrical structure of thunderclouds, namely, to the origination of the Lower Positive Charged Region (LPCR) below the main negative charged layer in the middle of the thundercloud, and to lightning occurrences. Only after creation of the lower dipole in the thundercloud can the electrons be accelerated and particle flux be directed downward. Maturity of the LPCR is correlated with increasing particle fluxes. Thus, the temporal evolution of TGE gives direct evidence of the maturity of LPCR, its initiation, and its decaying.

DOI: 10.1103/PhysRevD.86.072003 PACS numbers: 92.60.Pw, 52.38.Ph, 82.33.Xj, 93.30.Db

I. INTRODUCTION

Thunderstorms, because of their potential to kill and cause extensive property damage, are an important issue not only for researchers but also for society. However, in spite of many experimental and theoretical studies, the origin of electrification in clouds is still poorly understood; the layered structure of the thundercloud is variable and unexplained; and the relationship between electrification, lightning activity, and particle fluxes have not been unambiguously established [1].

Although there are big varieties of measures in the thundercloud electric field profiles, the following basic structure of the electric field in thunderclouds is widely accepted: from the ground up to the cloud base there is usually a low magnitude field (either positive or negative); a relatively small positively charged ''pocket'' is lowermost just at the cloud base (comprising only ~20% of a higher negative charge); a larger positive field prolongs up to the negative charge layer at 1–2 km above the cloud base; and about 1–4 km above the negative layer the main positive charge is located [2]. The Lower Positive Charge Region (LPCR) with a main negative layer in the middle of the cloud represents the so-called lower dipole, responsible for the downward electron acceleration and also playing a major role in the initiation of cloud-to-ground (CG −) and intracloud (IC −) lightning occurrences. LPCR is localized to a fairly small volume; therefore it should alter (at least locally) the electrical field at the ground. Holden *et al.* [3] concluded that the effect of the field attributable to LPCR's is usually only observable at distances less than 1 km.

The acceleration of electrons in the strong electric fields inside thunderclouds was postulated by Wilson [4] in 1924. In 1992 Gurevich *et al.* [5] developed the theory of the runaway breakdown, now mostly referred to as relativistic runaway electron avalanches (RREA) [6]. In [7] we consider the alternative mechanism of electron enhancement in thunderclouds, namely, the modification of energy spectra (MOS) of charged cosmic-ray particles [8]. Both scenarios lead to enhancements of the electrons and gamma rays in the thunderclouds, and if the height of clouds is not very large, particle detectors located on the Earth's surface can register enhancement of count rates of electrons and gamma rays, so-called Thunderstorm Ground Enhancements (TGEs), lasting as long as the lower dipole sustains electron acceleration. Various particle detectors (see Table I) of the Aragats Space Environmental Center (ASEC) [9,10] measure ~300 TGEs during springs and autumns of 2009–2012 in the fluxes of electrons, gamma rays, and neutrons.

It has been suggested that RREAs seeded by cosmic-ray extensive air showers (EASs) could result in enough ionization to initiate lightning [11,12]. However, Babich [13] and Dwyer and Babich [14] argue that lateral diffusion and the relativistic feedback threshold on the amount of

*chili@aragats.am

 © 2012 American Physical Society

TABLE I. Characteristics and parameters of ASEC particle detectors.

Detectors	Mean count rate per minute	10 MeV Gamma ray detection efficiency [%]	Electron detection threshold (efficiency)	Standard deviation and (relative standard deviation)	Percent of enhancement/ Number of standard deviations at 3:04 UT, May 11, 2012.
MAKET 5 cm thick 1 m^2 scintillator	26 400	1%	9 MeV (50%) 50 MeV (> 95%)	182 (0, 69%)	19%/28σ
STAND 3 cm thick 1 m^2 scintillator	32 800	4%	4 MeV (50%)	218 (0, 67%)	48%/72σ
STAND 100 combination	19 500	1%	2 MeV (50%)	160 (0, 82%)	60%/70σ
STAND 3 cm 1000 combination	6971	4%	4 MeV (50%)	93 (1, 33%)	60%/45σ
STAND 3 cm 1100 combination	3427	0.2%	15 MeV (50%)	57 (1, 65%)	33%/20σ
STAND 3 cm 1110 combination	2980	0.01%	25 MeV (50%)	57 (1, 91%)	10%/5σ
AMMM, 27 outside 5 cm thick, 1 m^2 scintillator	958 000	1%	9 MeV (50%) 50 MeV (> 95%)	1358 (0, 14%)	15%/110σ
NaI crystal, 12 × 12 × 24 cm	3678	85%	3 MeV (50%) 17 MeV (> 95%)	61 (1,67%)	33%/20σ
SEVAN, 5 cm thick 1 m^2 scintillator	26 600	4%	18 MeV (50%) 50 MeV (> 95%)	170 (0, 64%)	12%
SEVAN, 100 combination	17 800	4%	18 MeV (50%)	135 (0, 76%)	17%
SEVAN, middle, 20 cm thick 0.25 m^2 scintillator	7669, 6	0, 4%	100 MeV (50%) 350 MeV (> 95%)	88 (1, 15%)	5%
SEVAN 010 combination	2244, 5	0, 4%	100 MeV (50%)	43 (1, 9%)	13%

avalanche multiplication prevent a joint action of EASs and RREAs to initiate lightning. Nevertheless, they do not rule out that RREA acting on the ambient cosmic-ray flux could discharge the large scale electrical field in such a way that local electric field enhancements occur, potentially providing a high enough field region to allow lightning to initiate [15,16].

Additionally, Dwyer [1] pointed to the possibility that the gamma ray glows (the gamma ray component of the TGE) may be a manifestation of the steady state configuration of the electric field in which the charging currents are balanced by the discharge RREA currents. Lasting tens of minutes TGEs may affect lightning initiation, and research of the correlations of lightning and TGE can provide long missing clues to understand the lightning physics.

In this paper the correlations between thundercloud electrification (near-surface electrical field and type of lightning discharge) and measured particle fluxes were studied, thus invoking in the atmospheric electricity research a new type of key evidence—temporal evolution of the TGEs, the flux of gamma rays and electrons coming from thunderclouds and detected on the earth's surface by particle detectors [17,18]. For the first time we present simultaneous measurements of the particle fluxes, disturbances in the near-surface electrical field, and lightning initiations of different types.

II. THE LOWER POSITIVE CHARGE REGION (LPCR) AND ITS INFLUENCE ON THE NEGATIVE CLOUD-TO-GROUND (CG −) AND INTRACLOUD (IC −) LIGHTNING OCCURRENCES

During the past three years of TGE research on Aragats ~300 significant enhancements of particle detector count rates were detected. After locating the field meters and lightning detectors in 2010–2011, we found that all TGEs were accompanied by the disturbances of the near-surface electric field and most of them with lightning occurrences. We started with classification of TGEs according to patterns of near-surface electrical field disturbances. Then we examined each class to get evidence for how the particle flux increases and what happens with lightning occurrences as a flux is enlarged. Our model of TGE initiation [7,18] suggests that electron acceleration could start only after the creation of the LPCR below the main negative charged region in the center of the cloud. If the electric field between two differently charged regions is strong enough, the RREA process is unleashed and runaway electrons generate gamma rays; gamma rays in turn, if energetic enough, can generate neutrons via photonuclear reactions. If the electric field is below the RREA threshold, then only the MOS process can result in additional fluxes, although much weaker compared with RREA.

Simpson and Scrase [19] found that many thunderstorms contain a region of the positive charge located below the main negatively charged layer in the middle of a

thundercloud; they speculated that the positive charge resided on precipitation particles. Measurements by Holden *et al.* [3] show that LPCR's are not always found because they are localized to a fairly small volume and are transient phenomena as well. LPCR's are short-lived because, being composed of precipitation, they fall out of the cloud and carry their charge to the ground. As the LPCR approaches the ground, it should alter (at least locally) the field at the ground; thus LPCRs are responsible for the field reversals [20]. Many researchers outline the dominant role the lower positive charge region plays in initiating/triggering an intracloud and the cloud-to-ground lightning discharge [21–23]. The influence of the LPCR on lightning leader propagation can be considered in the following steps:

(a) While the negative charge accumulates at midlevel, it may not be energetically favorable to transfer the negative charge to ground in CG− lightning. Starting to develop a lower positive charge results in the enhancement of the electric field strength within the cloud and allows for negative charge transfer to ground in −CG lightning occurrence [24].

(b) When the size and magnitude of LPCR are becoming considerably large, the negative ("inverse"[1]) intracloud discharges IC− (attempted leader) are expected to occur. Because of screening the positive charge, the descending negative leader may change its direction of propagation to horizontal and end up as IC − .

Thus, the existence of the LPCR is a necessary condition for the TGE unleashing and, also, for the lightning initiation. At the initial stage of the LPCR developing or at the stage of LPCR decaying the cloud-ground CG− lightning occurrences should be often; in contrast, during the mature stage of LPCR CG− lightnings are blocked, and mostly intracloud IC− lightning should occur. An example of the above-described scenario gives lightning studies on the central Tibetan Plateau at an altitude of 4508 m. The IC− flashes registered on Tibet were usually polarity inverted and occurred in the lower dipole. The large LPCR did not cause positive CG+ flashes to occur during the whole storm lifetime, and only negative CG− flashes were observed in the late stage of the storm [25]. Also, the flash rate was quite low. It is worthwhile to note that recently the TGE detection on Tibet also was reported [26].

III. CHARACTERISTICS OF THE PARTICLE DETECTORS

Detection of the TGE events was made with particle detectors composed of plastic scintillators (see the description of the detector construction in [17]) and NaI crystals. Huge measured enhancements of the detector count rates are because both neutral and charged particles can generate signals in plastic scintillators, although with different efficiencies; see Table I. Therefore, to estimate energy spectra, we need to disentangle the mixture of electrons and gamma rays. Special experimental facilities were designed and installed at Aragats for separating electron and gamma ray fluxes. Two 20 cm thick plastic scintillators located inside the cube detector are completely surrounded by 1 cm thick molded plastic scintillators. Thick scintillators detect charged flux with very high efficiency (99%) and also neutral flux with efficiency 20%–30%. Thin scintillators also detect charged flux with very high efficiency (98%–99%), though the efficiency of detecting neutral flux is highly suppressed and equals 1%–2%. Using the advanced coincidences technique, it is possible to purify the neutral flux detected by inside scintillators, rejecting the charged flux by signals from surrounding thin scintillators. The calibration of the cube detector proves that the veto system (preventing the counting signal in the thick scintillator if there is a signal in at least one of the six surrounding thin scintillators) can reject 98% of the charged flux (see details in [7]). ASEC particle detectors are placed at high altitude, some of them under snow, and it is very difficult to keep a stable detector operation (high voltage, electronics thresholds, and other). However, high altitude station staff maintained detector operation 24 h daily for 12 months yearly, and online visualization programs ADAS [27] and ADEI [28] provide possibilities for the remote monitoring and control of the key parameters of detectors. All meteorological parameters, including atmospheric pressure are monitored; the barometric coefficients for all detectors are calculated and used for the count rate correction [29]. In Fig. 1 we post the characteristics of one of the recent TGE events and explain how we enumerate it. The minutely mean count rate (m), variance (σ), and relative error shown in the histogram agenda are calculated by the 3 h of fair weather data before TGE. The significance of peak at 3:04 Universal Time (UT) is enumerated in the so-called "number of sigmas," dividing the peak amplitude (48%) by relative error (0.66%).

In Table I we present the statistical characteristics of some of the ASEC detectors, demonstrating as well their measurement of the May 11 TGE. The count rate and variance depends on the size of the detector and the amount of matter above it. The highest enhancement demonstrated stacked 1 cm and 3 cm thick plastic scintillators, STAND and STAND 3 cm. STAND consists of 3 stacked 1 cm thick scintillators, and STAND 3 of 4 3 cm thick stacked scintillators of 1 m^2 area each. The 1000 abbreviation means that the signal comes only from the upper scintillator and the particle was stopped in it; 1100—signal measured from 2 upper scintillators, etc. The MAKET scintillators have a thickness of 5 cm, and they are located under metallic housing; therefore the threshold is higher and the enhancement is lower. The smallest relative error 0.14% (and

[1]The "normal" IC+ intracloud lightning occurs between main negative and positive layers of the dipole; the electric field is negative and electrons are accelerated upward.

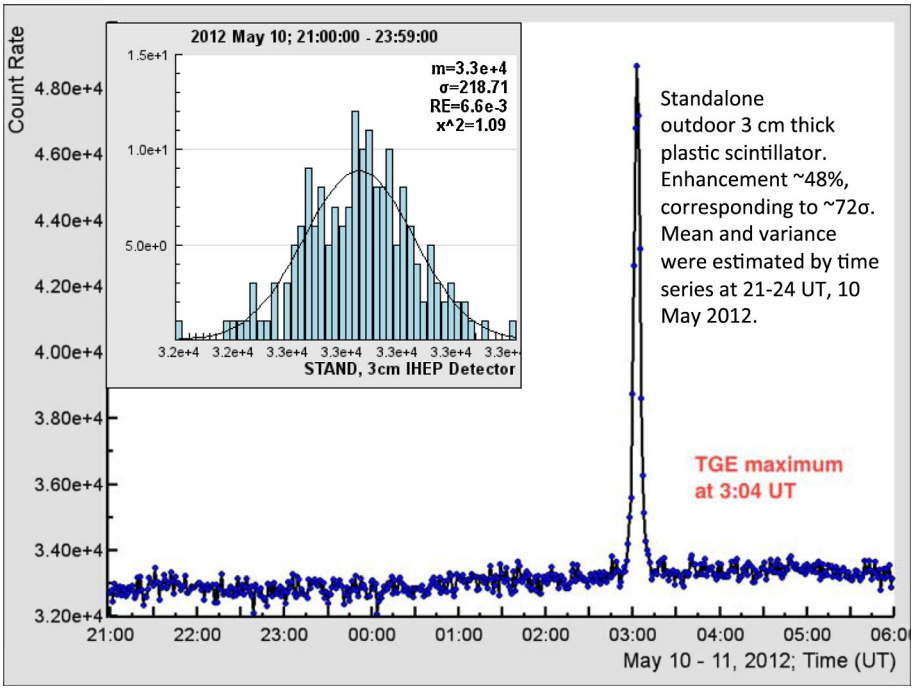

FIG. 1 (color online). Detection of the TGE occurred on May 11, 2012, by the outdoor 3-cm thick scintillator.

therefore largest significance 110σ) comprises from 27 m^2 area 5 cm thick scintillators; the largest relative error 2.06% from the NaI crystal of volume $13.5 \times 13.5 \times 21$ cm.

In Table I we present the energy thresholds of electron detection at 50% and 95% efficiency and efficiencies of gamma ray detection; note the very high efficiency of NaI crystals owing to ~5 radiation length thickness. The efficiency of particle detection by different combinations of stacked detectors allows the recovering of the energy spectra.

IV. CLASSIFICATION OF THE TGE EVENTS ACCORDING TO THE NEAR-SURFACE ELECTRICAL FIELD DISTURBANCES

Electric field meters[2] and lightning detectors (LD)[3] installed at Aragats as well as the multipurpose weather station[4] allow correlating TGEs with electric field disturbances, with occurrences of lightning of different types, and with other meteorological conditions (rain, atmospheric pressure, temperature, and humidity). LD's antenna consists of a crossed loop magnetic field sensor and electric field sensor. It records a signal when it detects an abrupt change in the electric field and can sense storms up to 350 miles away and can detect up to 3000 to 3500 strokes per second. For each lightning stroke, software analyzes a signal waveform in real time. To determine polarity (positive or negative) the software looks at the electric field at various points in the waveform. The discrimination between IC and CG is based on the shape and amplitude of the waveform, i.e., the rise and decline times, measured by the sensor through the change in electric field strength. These changes are strongest for CG discharges, where the decline time is the most important parameter; IC lightning generates much higher short-term energy at higher frequencies than CG strokes. When the electric field strength reaches a certain threshold value and rises further to a previously determined validation threshold, one can assume the electric field is attributable to a CG discharge. The direction is determined by looking at the magnetic field ratios for each stroke and crossed loop antenna direction finding principle. The initial distance is determined by looking at the signal strength. Software averages each stroke against a cluster of other strokes that are located toward the same direction, and from that derive a distance to the entire storm cell. Detection of the consequences of the IC− discharges without any CG discharge in the vicinity of the detector confirmed by the absence of lightning discharges from independent measurements of the EFM-100 electrical mill (the electrical mill detects only

[2]Boltek firm electrical mill EFM100, measurement accuracy 5%, http://www.boltek.com/efm100.html; Boltek firm adopted the atmospheric electricity sign convention, and we adopted apposite, physics sign convention; therefore, the negative sign of the electrical field measured by the Boltek electrical mill corresponds to the positive charge above.

[3]Boltek's StormTracker Lightning Detection System, powered by the software from Astrogenic systems, define four types of lightning occurrences (CG − , CG+ cloud-to ground negative and positive, IC − , IC_+ intracloud positive and negative, − in radii of 1, 3, and 5 km around the location of its antenna), http://www.boltek.com/stormtracker.

[4]Professional Davis Instruments Vantage Pro2, http://www.davisnet.com/.

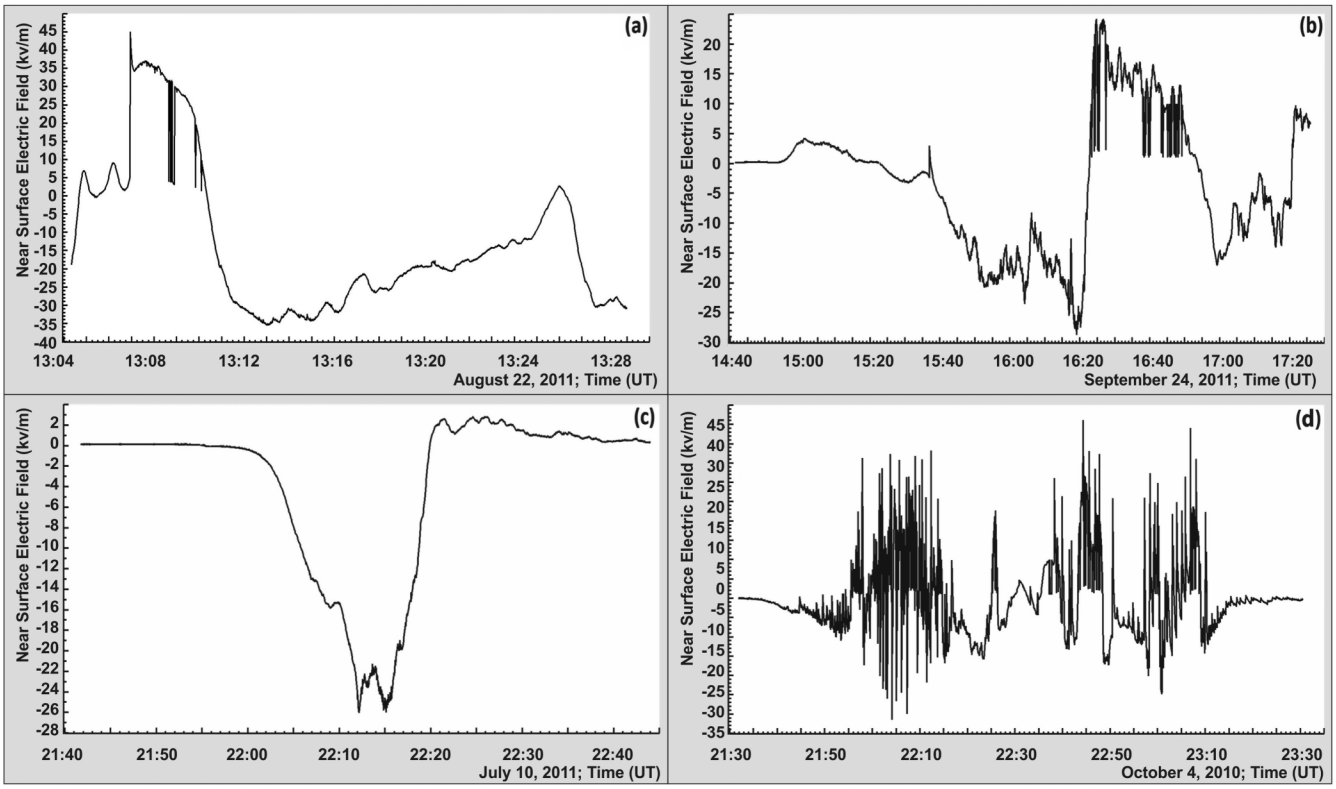

FIG. 2. Four patterns of the electric field disturbances during TGE events on Aragats.

cloud-to ground discharges) can be accepted as highly reliable. Also comparisons of measurements made by the network of three identical EFM-100 electrical mills prove reliability and high accuracy (not worse than 10%) of near-surface electric field estimation.

The TGE amplitude (the percentage of enhancement of particle flux relative to the rather stable background of secondary cosmic rays) was measured by the outdoor 3 cm thick, 1 m^2 area plastic scintillators and checked by other particle detectors; see Table I. Time series of particle intensity, electric field measurements, lightning occurrences, and meteorological information are entered in the MySQL database and are visualized with ADEI multivariate visualization code.[5] The joint database of the TGE events accompanied by electrical field and lightning occurrence measurements consists of 98 events detected from October 2010 to May 2012. Examining disturbances of the near-surface electric field, we outline the following most typical patterns accompanied with TGE (see Fig. 2):

(1) Electric field reversal from positive to negative [Fig. 2(a)]: field strength changes from a large (up to 50 kV/m) positive electric field to a low (down to −35 kV/m) negative value. We analyze six events (depicted in Tables II and III) of this type from 31, and an example of the first type of events is presented in Fig. 3.

(2) Electric field reversal from negative to positive [Fig. 2(b)]: changes from a low (down to −35 kV/m) negative electric field to a large positive electric field (∼ 50 kV/m). We analyze four events (depicted in the Tables IV and V) of this type from 11; an example of the second type of events is presented in Fig. 4.

(3) Electric field's abrupt decreases [Fig. 2(c)]: changes started from a fair weather value (few hundred volts) down to large negative values (− 30 kV/m); we select five events of this type from 28 (see Tables VI and VII); an example of the third type of events is presented in Fig. 5. We also include in this category events started from the intermediate positive electrical field (∼ 5 kV/m) and events having a large peak enhancement of electrical field in the middle of a negative electrical field period.

(4) Multiple disturbances of a near-surface electrical field [Fig. 2(d)] accompanied by numerous lightnings. We classify 28 events of the fourth category; analyses of these events will be published elsewhere.

Usually all four types of TGE events were accompanied with precipitation and lightning occurrences; however, sometimes lightning and rain are missing.

[5]ADEI (Advances Data Extraction Infrastructure) is an AJAX based dynamic web interface facilitating browsing and extraction time series from various data sources, http://adei.crd.yerphi.am/adei/.

TABLE II. First types of TGE events according to changing pattern of the near-surface electric field.

Date	Duration of positive field	Maximal value of electric field	Duration of negative field	Minimal value of electric field	FDHM of TGE	Flux increase (max flux minute)	Rain duration
04.10.10	18:14–18:20	28, 8 kV/m	18:20–18:25	−28, 8 kV/m	18:22–18:23	76%	Missing data
24.05.11	13:17–13:26	22, 15 kV/m	13:26–13:40	−35, 2 kV/m	13:29–13:38	3%	Missing data
27.05.11	13:05–13:10	45 kV/m	13:10–13:25	−35, 5 kV/m	13:11–13:16	21%	Missing data
08.06.11	11:44–11:52	38, 68 kV/m	11:54–12:18	−30, 95 kV/m	11:53–11:59	1, 7%	11:53–12:47
15.07.11	21:05–21:24	14, 05 kV/m	21:24–21:41	−29, 3 kV/m	21:26–21:35	2, 44%	No rain
22.08.11	22:06–22:14	17, 9 kV/m	22:14–22:25	−29, 95 kV/m	22:14–22:20	8%	22:16–23:09
20.09.11	10:09–10:20	21, 05 kV/m	10:20–10:40	−29, 45 kV/m	10:22–10:28	2, 55%	07:56–09:47

V. TGE EVENTS OF THE FIRST TYPE

During the first type of events (see Fig. 3), the near-surface positive electric field reaching a strength of 40 kV/m after a series of lightning occurrences (usually very few occurrences were distributed among intracloud positive and negative lightning IC+ and IC− and cloud-to-ground lightnings CG − ; see Table III) started to reverse, and simultaneously particle flux started to slowly rise at 13:10 UT. During the long period of negative near-surface electric field, we suppose that the larger in dimension and higher in charge magnitude LPCR developed at the base of the storm and electrons are accelerated downward by the lower dipole. Lasting ∼10 min the negative near-surface electric field coincides in time with large particle flux; the developed LPCR creates a larger positive electric field in the cloud that increases the particle flux downward, peaking at ∼13:13 UT when the negative field approaches the minimal strength of −35 kV/m. During several minutes of particle flux maximum IC+ and CG− lightning occurrences are highly suppressed and only IC− lightnings were observed. Emerging large LPCR blocks the step leader propagation to the ground and turns it to intracloud IC− flash because the abundant lower positive charge made IC discharges energetically preferable. At 13:20 UT the LPCR contracted and particle flux decayed. Consequently diminished LPCR cannot block the lightning leader propagation to the ground any more, and several CG− lightnings occurred at 13:23 UT at the fully stopped particle flux.

The information on the first type of TGEs is posted in Table II. TGE duration comprises ∼10 min; however, sometimes we detect long lasting tails of particle fluxes. To avoid possible ambiguity, we ''normalize'' the TGE duration by calculating the full duration of the TGE peak on the half-maximum (FDHM). In the first, second, and fourth columns we post the date of the TGE event and durations of the positive and negative fields; in the third and fifth columns we show the maximal and minimal values of the near-surface electrical field; the FDHM of the TGE peak and TGE amplitudes are presented in the sixth and seventh columns. In the last column we show information on rain; missing data denote the absence of the rain measurements. As we see in Table II, the range of the

TABLE III. Fractions of lightning occurrences of different types during positive and negative (FDHM) near-surface electric fields.

	Fraction of lightnings of different types within 1 km					Fraction of lightnings of different types within 3 km					Fraction of lightnings of different types within 5 km				
Date	Flash rate	IC−	IC+	GC−	GC+	Flash rate	IC−	IC+	GC−	GC+	Flash rate	IC−	IC+	GC−	GC+
04.10.2010 Duration of positive field (18:14–18:20 UT)	0/ min	0%	0%	0%	0%	0, 17/ min	0%	100%	0%	0%	0, 5/ min	66, 7%	33, 3%	0%	0%
04.10.2010 FDHM of TGE (18:22–18:23 UT)	1/ min	100%	0%	0%	0%	2/ min	100%	0%	0%	0%	9/ min	100%	0%	0%	0%
27.05.2011 Duration of positive field (13:05–13:10 UT)	2, 2/ min	27%	55%	18%	0%	12, 6/ min	36%	40%	24%	0%	16, 2/ min	30%	39%	31%	0%
27.05.2011 FDHM of TGE (13:11–13:16 UT)	0, 4/ min	100%	0%	0%	0%	28, 2/ min	97%	3%	0%	0%	106, 2/ min	84%	15%	1%	0%
22.08.2011 Duration of positive field (22:06–22:14 UT)	0/ min	0%	0%	0%	0%	0/ min	0%	0%	0%	0%	0/ min	0%	0%	0%	0%
22.08.2011 FDHM of TGE (22:06–22:20 UT)	15/ min	100%	0%	0%	0%	20/ min	100%	0%	0%	0%	22/ min	100%	0%	0%	0%

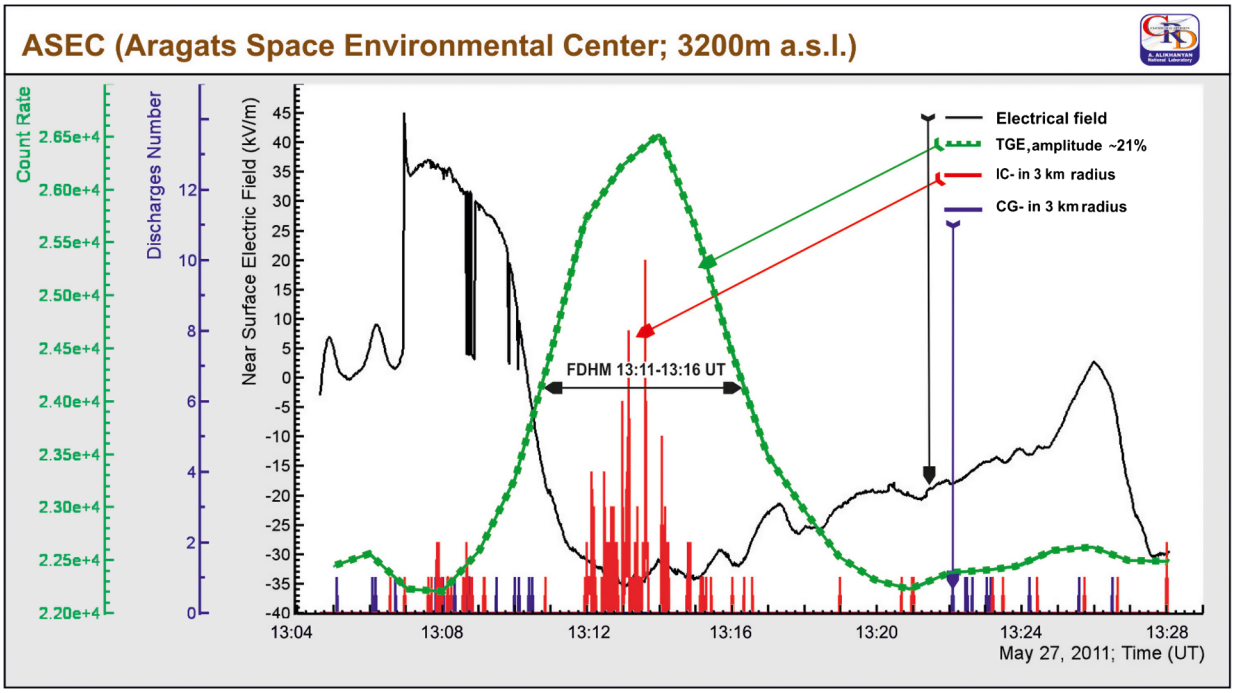

FIG. 3 (color online). TGE of the first type according to the pattern of the electric field disturbances; the black curve shows the changing electric field; the gray dotted curve shows the time series of the particle flux. Vertical gray lines denote IC− lightning and vertical darker lines CG− lightning occurrences within 3 km radius.

maximal values of the positive electric field varies 14–45 kV/m, duration 5–20 min. The maximal value of the negative field changes from −28 to −35 kV/m, duration 5–20 min. TGE amplitude changes from 2.5% to 76%, and the FDHM is shorter than negative field duration and continues usually 4–9 min, although only once does it fall to 1 min for the super TGE on October 4, 2010.

TABLE IV. Second types of TGE events according to changing pattern of the near-surface electric field.

Date	Duration of negative field	Minimal value of electric field	Duration of positive field	Maximal value of electric field	FDHM of TGE	Flux increase (max flux minute)	Rain duration
13.07.11	00:51–01:17	−26, 55 kV/m	01:17–01:36	24, 7 kV/m	01:06–01:11	3, 92%	00:59–01:47
24.09.11	15:37–16:22	−28, 6 kV/m	16:22–16:53	24 kV/m	16:11–16:20	8, 05%	15:17–16:26
25.09.11	11:31–11:53	−32 kV/m	11:53–12:09	12 kV/m	11:38–11:47	3, 74%	11:58–12:37
17.10.11	13:41–14:01	−18 kV/m	14:01–14:07	25 kV/m	13:50–13:56	2, 82%	no rain

TABLE V. Fractions of lightning occurrences of different types during positive field and FDHM of TGE.

	Fraction of lightnings of different types within 1 km					Fraction of lightnings of different types within 3 km					Fraction of lightnings of different types within 5 km				
Date	Flash rate	IC−	IC+	GC−	GC+	Flash rate	IC−	IC+	GC−	GC+	Flash rate	IC−	IC+	GC−	GC+
13.07.2011 FDHM of TGE (01:06–01:11 UT)	0/ min	0%	0%	0%	0%	0, 2/ min	100%	0%	0%	0%	0, 8/ min	100%	0%	0%	0%
13.07.2011 Duration of positive field (01:17–01:36 UT)	0/ min	0%	0%	0%	0%	0/ min	0%	0%	0%	0%	0/ min	0%	0%	0%	0%
24.09.2011 FDHM of TGE (16:11–16:20 UT)	69/ min	96%	1%	3%	0%	93, 78/ min	94%	2%	3%	1%	100, 5/ min	92%	3%	4%	1%
24.09.2011 Duration of positive field (16:22–16:53 UT)	3, 45/ min	40%	35%	20%	6%	15, 9/ min	52, 2%	23, 3%	21, 1%	3, 4%	24/ min	47%	27%	22%	4%

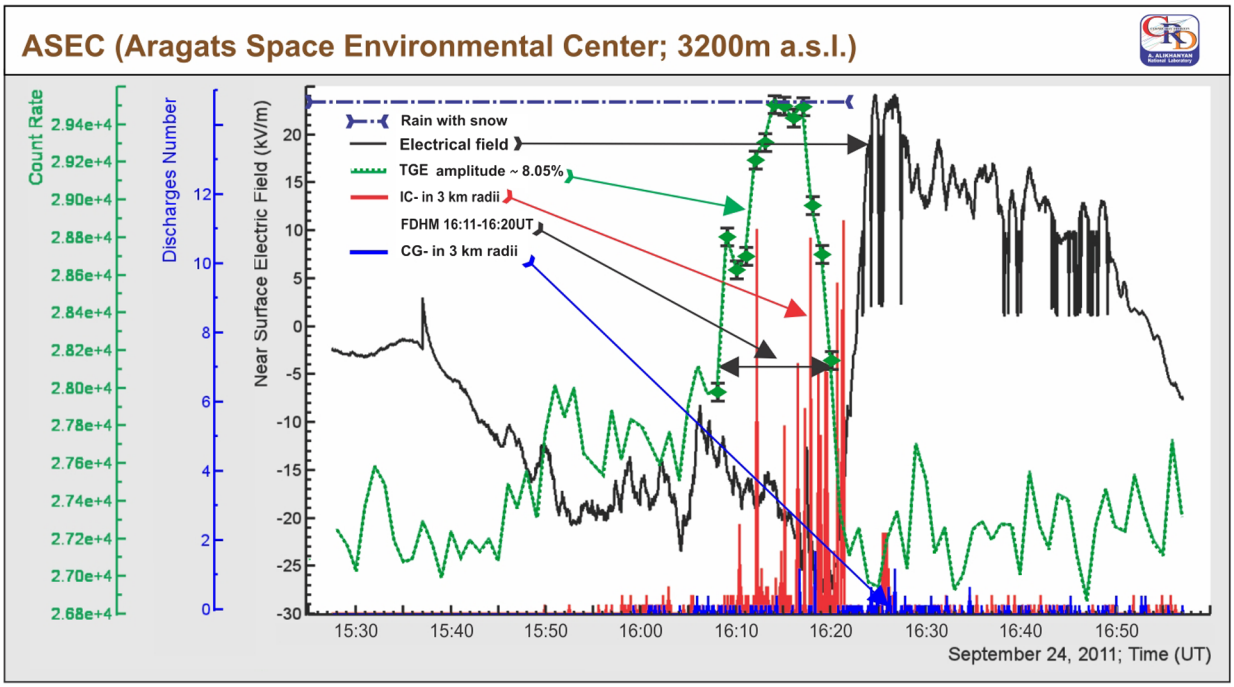

FIG. 4 (color online). TGE of the second type according to the pattern of the electric field disturbances; the black curve shows the changing electric field; the gray dotted curve shows the time series of the particle flux. Vertical gray lines denote IC− lightning and vertical darker lines CG− lightning occurrences within 3 km radius.

In the first column of Table III we post the date of the event and duration of the positive field and negative (FDHM) electrical field; in the second–fifth columns we show the flash rate (number of lightning occurrences per minute) and fractions of lightnings of different types during positive and negative fields (FDHM) in 1 km radius from detector location. The same information on frequency of lightnings for the radii 3 and 5 km is posted in the next columns. The pattern of frequencies is drastically different. If at the positive field the share of three types of lightning occurrences (intracloud positive and negative and cloud-to-ground negative) is approximately equal, at the negative field during FDHM we detect strong suppression of CG− and IC+ lightning occurrences (positive cloud-to-ground lightning IC+ is a rather rare occasion). In the vicinity of particle detectors in a 1 km radius we detect only IC− lightnings, and when enlarging the radius around the detection site other types of lightnings occur; however, their fraction was negligible, only once reaching 20% (IC+ type at May 24, 2011, in 3 km radius). The mean flash rate during TGE FDHM is very moderate within a 1 km radius ranging from 0 to 1.5, confirming the results of the Tibet Plateau lightning occurrences study [23,25] in a 3 km radius, the rate is significantly larger: from 0.56 to 28.2. This finding supports recent results of the Japanese groups measuring the size of the radiation region within the thundercloud to be not more than 1 km [30,31].

VI. TGE EVENTS OF THE SECOND TYPE

During the second type of the TGE events (see Fig. 4), the near-surface electric field gradually decreases from the near-zero value at 15:40 UT and remains in the negative domain near 40 min. At 16:10–16:22 UT particle flux

TABLE VI. Third types of TGE events according to changing pattern of the near-surface electric field.

Date	Duration of negative field	Minimal value of electric field	FDHM of TGE	Flux increase (max flux minute)	Rain duration
07.05.11	20:35–21:30	−34, 5 kV/m	21:11–21:15	4, 36%	Missing data
08.05.11	01:43–02:09	−32 kV/m	01:45–01:51	7, 5%	Missing data
12.06.11	09:11–10:15	−26, 75 kV/m	10:00–10:09	5, 17%	10:38–11:11
10.07.11	21:56–22:20	−26, 05 kV/m	22:10–22:15	4, 36%	22:15–22:35
13.10.11	11:24–11:50	−29, 5 kV/m	11:32–11:39	12%	No rain
16.10.11	23:59–00:14	−17, 35 kV/m	00:08–00:12	8, 83%	No rain
25.10.11	23:08–23:37	−18, 55 kV/m	23:24–23:33	2, 27%	No rain

TABLE VII. Fractions of lightning occurrences of different types at FDHM of TGE.

Date	Fraction of lightnings of different types within 1 km					Fraction of lightnings of different types within 3 km					Fraction of lightnings of different types within 5 km				
	Flash rate	IC−	IC+	GC−	GC+	Flash rate	IC−	IC+	GC−	GC+	Flash rate	IC−	IC+	GC−	GC+
07.05.11 FDHM of TGE (21:11–21:15 UT)	58, 75/ min	96, 2%	21, 27%	1, 07%	0%	250, 5/ min	98%	1%	0%	0%	272, 25/ min	98, 2%	1, 3%	0%	0%
08.05.11 FDHM of TGE (01:45–01:51 UT)	1/ min	50%	0%	50%	0%	26, 17/ min	92%	1%	6%	1%	44, 3/ min	93%	1%	5%	1%
12.06.11 FDHM of TGE (10:00–10:09 UT)	4, 11/ min	38%	43%	19%	0%	15, 9/ min	67%	17%	13%	3%	32, 11/ min	73%	14%	11%	2%
10.07.11 FDHM of TGE (22:10–22:15 UT	1, 6/ min	100%	0%	0%	0%	10/ min	74%	26%	0%	0%	46, 8/ min	62%	38%	0%	0%
13.10.11 FDHM of TGE (11:32–11:39 UT)	14, 7/ min	100%	0%	0%	0%	16/ min	100%	0%	0%	0%	16, 43/ min	99%	0%	0%	0%

reaches a maximum of 8%, the electric field peaks −28 kV/m at 16:19 UT, and simultaneously we observe highly enlarged lightning occurrences (see Fig. 4), mostly of the IC− type, and CG− lightning occurrences again were suppressed. At 16:24 UT an abrupt reversal of the field occurs, and the positive field peaked on 24.2 kV/m at 16:26 UT. The pattern of the lightning occurrences changed accordingly; see Tables IV and V.

We analyze four events of the second type (from 11) (see Table IV); the table information is the same as Table II. All three TGE started during the negative field; the field strength is changing from −32 to −18 kV/m; and the duration range is 20–45 min. The range of the positive electric field is 12–25 kV/m, with a duration of 7–30 min. TGE amplitude changes from 2.8% to 8%, and FDHM changes from 7 to 9 min. The rain started during the negative field and ended with TGE fading.

Very large numbers of lightnings were registered on September 24, 2011; a considerable fraction was registered in the minute of the peak of the particle flux, but most of them were IC − . Depending on the distance, fractions of lightnings changed insignificantly. In the vicinity of

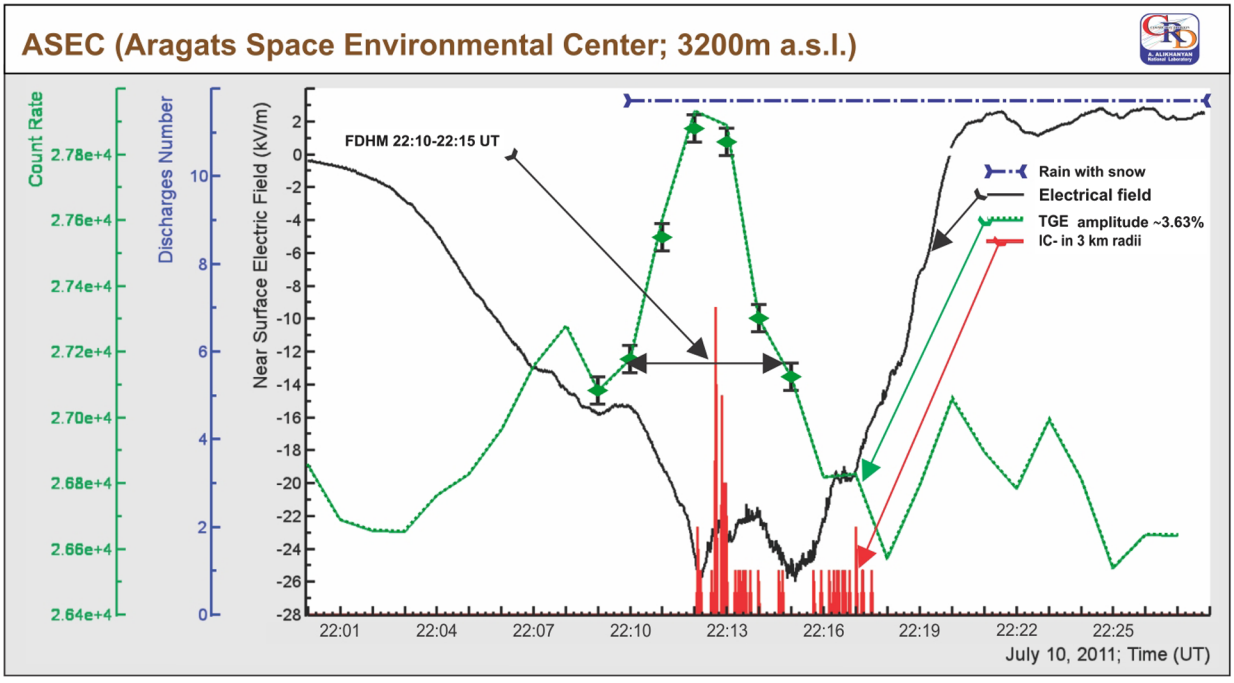

FIG. 5 (color online). TGE of the third type according to the pattern of the electric field disturbances; the black curve shows the changing electric field; the gray dotted curve shows the time series of the particle flux. Vertical gray lines denote IC− lightning occurrences within 3 km radius. Rain was detected during 22:15–22:35 UT.

particle detectors we detect plenty of the IC− lightnings; with enlarging of the radius other types of lightnings occur. On September 24, 2011, during the negative field we registered a large number of IC− lightnings; however, during the positive field we did not register any lightning. On this day the rain started during the positive field. Numbers of lightning occurrences of all types increased with the growth of the distance to the particle detectors.

VII. TGE EVENTS OF THE THIRD TYPE

During the third type of events (see Fig. 5), the near-surface electric field gradually decreases from the near-zero value at 22:00 UT and remains in the negative domain near 20 min, peaking at −26 kV/m on 22:12 and 22:15 UT; the particle flux starts to rise and peaks at 3.6% on 22:13 UT. After the start of the rain, the negative field returns very quickly to the near-zero value, and consequently the particle flux stopped.

IC− lightning occurrences started at the maximum of particle flux and continued till the flux faded. CG− lightning occurrences were not detected; IC+ lightnings occurred within 3 km radius around the particle detector location (see Table VII).

The third type of TGEs differs from the others as lightnings were registered only during the particle flux. We analyze five events of the third type from 28, and during some of them a large number of lightnings were registered (see Tables VI and VII).

As we see in Table VI, the value of the negative electric field varies from −34.5 to −18 kV/m, and the duration was 25–55 min. TGE amplitude changes from 2.27% to 12%, and FDHM of TGE varies from 4 tol 9 min. In two events we detected 100% IC− lightnings in 1 and 3 km radius. During the other events, the fraction of IC− lightnings also predominate, and lightning occurrences of CG− and IC+ were suppressed.

Table VII presents frequencies of lightning occurrences around the minute of maximal flux of TGE. In 1 km radius we detected only IC − ; with enlarging the radius around the detection, as we see, IC+ lightnings occur also.

VIII. CONCLUSION

Incorporation of the information on the changing particle fluxes measured during thunderstorms proves the model of LPCR as it was formulated in points (a) and (b) of Sec. II. LPCR and the lower dipole are transient and local phenomena; LPCR is created during minutes, with consequent acceleration of electrons in the lower dipole resulting in enlarged particle flux (TGE). Particle flux is a measure of the LPCR maturity; it reaches maximum at the largest LPCR size and decays on LPCR contracting fully agreeing with foundlings made in Tibet [23,25]. The negative polarity of the electric field signals that the LPCR is creating, and with developing LPCR the particle flux has consequently been rising; simultaneously mature LPCR prevents negative CG− flashes owing to an abundant lower positive charge making intracloud IC− flashes preferable (see also [22]). The negative CG− discharges occurred in the late stage of the storm on the degradation of the LPCR when the particle flux stopped. Therefore, scenarios (a) and (b) of Sec. II are enabled successively during one and the same thunderstorm. Aragats thunderstorm data also confirm the finding from Tibetan thunderstorms that emerged LPCR did not cause positive CG+ flashes. The characteristic time scale of maturing the LPCR is ∼10 min coinciding with estimates from thunderstorms at the Tibet Plateau.

The technique of measuring particle fluxes simultaneously with near-surface electric field and lightning occurrences of different types first developed and used on Aragats allows following up on the creation of the LPCR and its contraction. The maximal flux of gamma rays detected at the surface (and corresponding maximal flux of the electrons within the lower dipole) pointed at the maximal positive electric field in the cloud and, correspondingly, on the maximal dimension and charge of the LPCR. The distance between the main negatively charged layer in the middle of a cloud and LPCR should be significantly large to provide the large potential drop necessary for the electron acceleration. Fading of the gamma ray flux evidences the degradation of the LPCR. Measured particle flux along with registered lightning occurrences of the different types allows research of the fine structure of the thunderstorm, including the time evolution of the LPCR and ongoing processes of intracloud lightning initiation and electron avalanche propagation.

In several events the particle fluxes (TGEs) precede lightning occurrences, thus demonstrating that the downward moving streamer can use the conductive channel opened by the downward electron-gamma ray avalanche (see [32]); however, for some of the TGEs the frequency of lightning occurrences at maximal particle flux is very low, signaling that in some circumstances the particle acceleration and IC− lightning occurrences can compete.

ACKNOWLEDGMENTS

The authors highly appreciate the discussions of the topics related to the presented paper at seminars of the Cosmic-Ray Division of Alikhanyan National Lab. Arakelyan Karen and Pokhsraryan David were instrumental in installing and preparing software for treating the time series of electric field and lightning measurements. Reymers Artur provides data transfer from the particle detectors to databases at CRD headquarters. Suren Chilingaryan tuned ADEI data visualization code for cosmic-ray monitoring. Narine Khachatryan designed figures. To all of them the authors express gratitude for fruitful collaboration.

[1] J. R. Dwyer, D. M. Smith, and S. A. Cummer, Space Sci. Rev., doi: 10.1007/s11214-012-9894-0 (2012).

[2] M. Stolzenburg, T. C. Marshall, and W. D. Rust, J. Geophys. Res. **103**, 14079 (1998).

[3] D. N. Holden, C. R. Holmes, C. B. Moore, W. P. Winn, J. W. Cobb, J. E. Griswold, and D. M. Lytle, *Local Charge Concentration in Thunderclouds, in Sixth International Conference on Atmospheric Electricity* (University of Manchester, Manchester, England, 1980).

[4] C. T. R. Wilson, Proc. Cambridge Philos. Soc. **22**, 534 (1925).

[5] A. V. Gurevich, G. M. Milikh, and R. A. Roussel-Dupré, Phys. Lett. **165A**, 463 (1992).

[6] L. P. Babich, I. M. Kutsyk, E. N. Donskoy, and A. Y. Kudryavtsev, Phys. Lett. A **245**, 460 (1998).

[7] A. Chilingarian, B. Mailyan, and L. Vanyan, Atmos. Res. **114–115**, 1 (2012).

[8] L. I. Dorman and I. V. Dorman, Adv. Space Res. **35**, 476 (2005).

[9] A. Chilingarian *et al.*, Nucl. Instrum. Methods Phys. Res., Sect. A, **543**, 483 (2005).

[10] A. Chilingarian *et al.*, J. Phys. G **29**, 939 (2003).

[11] A. V. Gurevich and G. M. Milikh, Phys. Lett. A **262**, 457 (1999).

[12] A. V. Gurevich, L. M. Duncan, A. N. Karashtin, and K. P. Zybin, Phys. Lett. A **312**, 228 (2003).

[13] L. P. Babich, E. I. Bochkov, and I. M. Kutsyk, Geomagn. Aeron. **49**, 232 (2009).

[14] J. R. Dwyer and L. Babich, J. Geophys. Res. **116**, A09301 (2011).

[15] J.R . Dwyer and D. M. Smith, Geophys. Res. Lett. **32**, L08811 (2005).

[16] L. P. Babich, E. I. Bochkov, and I. M. Kutsyk, J. Exp. Theor. Phys. **112**, 902 (2011).

[17] A. Chilingarian, A. Daryan, K. Arakelyan, A. Hovhannisyan, B. Mailyan, L. Melkumyan, G. Hovsepyan, S. Chilingaryan, A. Reymers, and L. Vanyan, Phys. Rev. D **82**, 043009 (2010).

[18] A. Chilingarian, G. Hovsepyan, and A. Hovhannisyan, Phys. Rev. D **83**, 062001 (2011).

[19] G. Simpson and F. J. Scrase, Proc. R. Soc. A **161**, 309 (1937).

[20] C. B. Moore and B. Vonnegut, *The Thundercloud, in Lightning*, edited by R. H. Golde (Academic, New York, 1977).

[21] S. D. Pawar and A. K. Kamra, J. Geophys. Res. **109**, D02205 (2004).

[22] A. Nag and V. A. Rakov, Geophys. Res. Lett. **36**, L05815 (2009).

[23] X. Qie, T. Zhang, C. Chen, G. Zhang, T. Zhang, and X. Kong, Atmos. Res. **91**, 244 (2009).

[24] E. R. Williams, M. E. Weber, and R. E. Orville, J. Geophys. Res. **94**, 13213 (1989).

[25] X. Qie, T. Zhang, G. Zhang, T. Zhang, and W. Wei, Geophys. Res. Lett. **32**, L05814 (2005).

[26] P. Salvini, *Proceedings of the workshop, Aragats-2011, Nor Amberd, Armenia* (Cosmic Ray Division, Yerevan Physics Institute, Yerevan, Armenia, 2012).

[27] S. Chilingaryan, A. Chilingarian, V. Danielyan, and W. Eppler, J. Phys. Conf. Ser. **119**, 082001 (2008).

[28] S. Chilingaryan, A. Beglarian, A. Kopmann, and S. Voekling, J. Phys. Conf. Ser. **219**, 042034 (2010).

[29] A. Chilingarian and T. Karapetyan, Adv. Space Res. **47**, 1140 (2011).

[30] H. Tsuchiya, T. Enoto, S. Yamada, T. Yuasa, K. Nakazawa, T. Kitaguchi, M. Kawaharada, M. Kokubun, H. Kato, M. Okano, and K. Makishima, J. Geophys. Res. **116**, D09113 (2011).

[31] T. Torii, T. Sugita, M. Kamogawa, Y. Watanabe, and K. Kusunoki, Geophys. Res. Lett. **38**, L24801 (2011).

[32] D. M. Smith, B. J. Hazelton, B. W. Grefenstette, J. R. Dwyer, R. H. Holzworth, and E. H. Lay, J. Geophys. Res. **115**, A00E49 (2010).